Mechanical reliability evaluation of silicon nitride ceramic components after exposure in industrial gas turbines

H.T. Lin*, M.K. Ferber

Metals and Ceramics Division, Oak Ridge National Laboratory, Oak Ridge, TN 37831-6068, USA

Abstract

Several studies have recently been undertaken to examine the mechanical reliability and thermal stability of silicon nitride ceramic components that are currently being considered for structural application in industrial gas turbines. Specifically, ceramic components evaluated included a bow-shaped silicon nitride nozzle evaluated in an engine test rig, silicon nitride vanes exposed in an engine field test, and an air-cooled silicon nitride vane that is currently under development. Despite the differences in field test conditions all of the exposed silicon nitride ceramic components exhibited a significant material recession arising from the oxidation of silicon nitride and subsequent volatilization of the oxide (i.e., silica). The fracture strength of exposed airfoils was also decreased due to the formation of a subsurface damage zone induced by the turbine environments. In addition, studies indicated that the properties of as-processed ceramic components, especially in airfoil regions, were not always comparable to those generated from the standard specimens with machined surface extracted from production billets. The component characterization efforts provided an important insight into the effect of gas turbine environments on the material recession and mechanical reliability of materials as functions of exposure time and conditions, which were very difficult to obtain from a laboratory scale test. © 2002 Elsevier Science Ltd. All rights reserved.

Keywords: Ceramic components; Gas turbines; Mechanical reliability; Si_3N_4

1. Introduction

Over the last 30 years, a number of programs in the United States have sought to introduce monolithic ceramic components into gas turbines with the goals of increasing efficiency and lowering emissions. High performance silicon nitride and silicon carbide ceramics typically have been leading candidates for use in these applications. In spite of their potential, ceramic components, especially silicon-based ceramics, exposed in engine tests have not exhibited the required reliability and stability.[1–3] One factor for this limited success is that the standard test specimens used to establish a database for life prediction generally are not fabricated in the exact same way as the turbine components. Consequently the properties measured in the laboratory may not truly reflect those of the components manufactured in the production line. For example, silicon

nitride ceramic components (particularly airfoils) contain as-processed surfaces, which may exhibit dramatically different properties compared with the bulk material due to the differences in microstructure and chemical composition. For thin sections these properties will ultimately govern the long-term mechanical reliability and lifetime of the components. In the case of silicon nitride ceramics, processing (green-state forming and high-temperature densification) of the complex-shaped components and laboratory tested simple-shaped specimens may be different, resulting in a significant difference in the high temperature mechanical performance.[4]

The second factor involves the deleterious effects of the gas turbine environments upon the stability and lifetime of silicon nitride ceramic components. In such environments, three processes can impact the performance and lifetime of the silicon nitride: (1) localized corrosion due to the presence of reactive species in the environment, (2) environmentally-induced destabilization of the secondary phases, and (3) rapid recession of the silicon nitride (also silicon carbide) due to the loss of

* Corresponding author. Tel.: +1-865-576-8857; fax: +1-865-574-8445.

E-mail address: linh@ornl.gov (H.T. Lin).

a protective silica scale by direct reaction with the water vapor. Localized corrosion can occur when metallic impurities, such as iron or nickel from metallic components in the engine, are deposited on the airfoil surface. The oxidation of these impurities disrupts the silica scale leading to the formation of surface corrosion pits. Environmental attack can also result in transformations of secondary phase(s) in subsurface region that give rise to stresses large enough to nucleate cracks.[5] Oxidation of both silicon nitride and silicon carbide is increased by the replacement of oxygen by water vapor and an increase in the pressure of the oxidant. In addition, the high velocities and presence of water in the environment can lead to the volatilization of the normally protective silica layer. Research carried out at NASA Glenn Research Center and Oak Ridge National Laboratory has shown that the presence of water vapor leads to the formation of a gaseous $Si(OH)_4$ species via a reaction with the silica layer.[6–11] The rate of formation, k, of this species and thus the rate at which the SiC (or Si_3N_4) is consumed by its continued oxidation is determined by the expression,

$$k \propto v^{1/2}P(H_2O)^2/(P_{total})^{1/2} \tag{1}$$

where v is the gas velocity, $P(H_2O)$ is the partial pressure of the water vapor, and P_{total} is the total pressure. For lean burn conditions, k for a number of SiC based materials is found to be well described by the expression,

$$k(mg/cm^2 \ h) = 2.04 \ exp(-108 \ kJ/mol/RT)v^{1/2}P_{total}^{3/2} \tag{2}$$

where T is the absolute temperature (K), P_{total} is the total pressure (atm), and v is the velocity (m/s). In addition to the volatility issues, which may lead to loss of function due to excessive changes in component dimensions, the effect of gas turbine environments upon the mechanical stability and performance must be understood as well.

A major issue with these environmental effects is that they are not easily reproduced in the laboratory. Although it is possible to conduct mechanical tests under conditions of high-pressure and high-temperature water vapor, representative gas turbine velocities were very difficult to obtain. Burner rigs are capable of generating both high-pressure and high-velocities, but they generally do not have provisions for applying controlled mechanical stresses that components would be subjected to during engine operation. One novel approach for avoiding the problems arising from material variations (between standard test specimens and the component) is to evaluate the component properties directly using small, specialized test specimens. For curved airfoil surfaces, miniature disks, which are prepared by diamond core drilling and back machining, can be used to quantify

the retained strength of airfoils. Sectioning of components that have been exposed in engine test rigs or field tests also provides quantification of time-dependent changes of thermal and mechanical properties. Extensive microstructural evaluation can be used to further define the effect of environment and service conditions on the mechanical reliability. This paper summarizes results of component characterization studies implemented in support of recent programs at Solar Turbines, Rolls-Royce, and Pratt & Whitney.

2. Experimental procedures

The first characterization method involved dimensional inspection of the ceramic vanes removed during the periodic field inspections. Specifically, the thickness of the trailing edge was measured at the tip, mid-span, and vane hub using a micrometer. Following completion of the field test all remaining vanes were measured in this manner. In addition, a few selected vanes were dimensionally inspected with a coordinate measuring machine (CMM). Here the primary emphasis was to measure changes in the shape of the mid-span slice of the airfoil.

X-ray diffraction analysis was used to identify the predominant secondary phases in the airfoil as a function of engine exposure time. For each airfoil examined, diffraction traces were obtained for the platform surface as well as the convex and concave sides of the airfoil. Scanning electron microscopy (SEM) was used to examine the surfaces of the airfoils and platforms after removal of the vanes from the engine. Selected vanes were subsequently sectioned and prepared for microstructure analysis using SEM.

The biaxial flexure strength[12–14] was measured for selected vanes using the ball-on-ring arrangement shown in Fig. 1. Specimens were machined from both the airfoil and platform surfaces by first diamond core drilling small cylinders having nominal diameters of 5.5 mm. Each cylinder was then machined on one face only until the thickness was 0.4–0.5 mm. In this way, one face of each specimen always consisted of the exposed surface of either the airfoil or platform. During testing, this surface was loaded in tension. The test fixture consisted of a 1.0 mm diameter hardened steel ball, which was mounted to a miniature load cell. The lower support ring, which was 5.0 mm in diameter, was fabricated from a high-strength polymer. It was mounted to a vertical stepper motor (Z stage), which was affixed to X–Y stages for positioning in the horizontal plane. A computer controlled all three stages. After placing a specimen on the lower support ring, the X–Y stages were used to position the assembly directly under the upper load ball. The Z-stage was then raised at a rate of 0.5 mm/s until the specimen made light contact with the
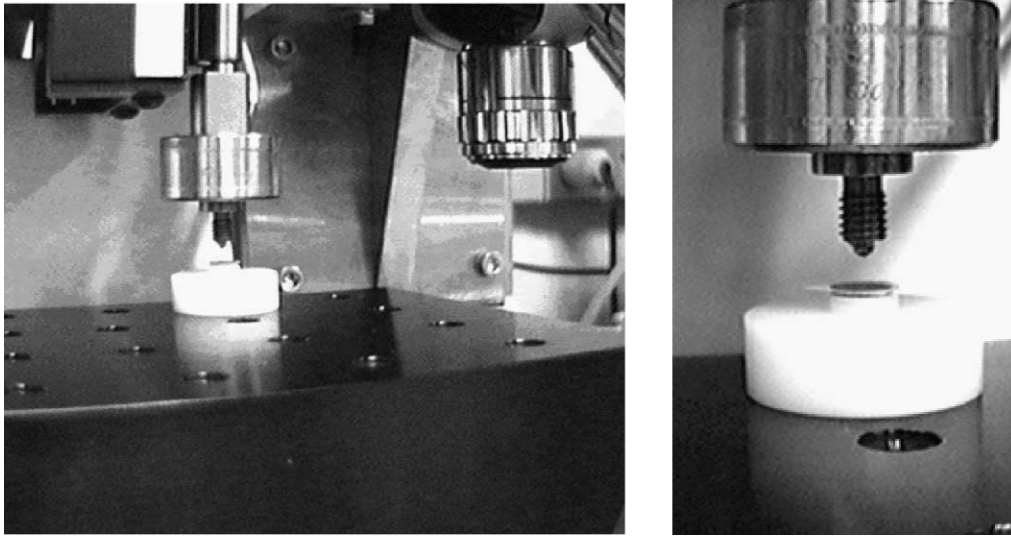
Fig. 1. Biaxial test fixture and specimen.

ball. The specimen was subsequently loaded to failure at a displacement rate of 0.05 mm/s. The computer monitored and recorded the displacement, load, and time.

The strength, S_b, was calculated from the equation

$$S_b = 3P(1 + n)/(4nt^2) \bullet [1 + 2\ln(a/b) + ((1 - n)/(1 + n))(1 - b^2/2a^2)(a^2/R^2)]$$ (3)

where P is the ultimate sustained load, a is the radius of the support "ring", b is the effective radius of contact of the loading ball on the specimen, R is the specimen radius, t is the specimen thickness, and v is Poisson's ratio. As a first approximation, b was taken as $t/3$.

3. Results and dicussion

3.1. Solar turbines

Solar Turbines was awarded the Ceramic Stationary Gas Turbine (CSGT) Development contract from the US Department of Energy (DOE) in 1992.[15] The goals of this program, which continued through 2000, were to improve engine performance (fuel efficiency and output power) and reduce exhaust emissions. The approach involved retrofitting an existing gas turbine (Solar's Centaur 50S, 4.1 MW) with silicon nitride nozzles (vanes), silicon nitride blades, and SiC fiber-reinforced SiC-based ceramic matrix composite combustor liner.

In September 1998, a 100-h nozzle engine test was initiated in which the engine was subjected to cold and hot engine restarts and shutdown cycles that progressively increased in severity. The nozzles were fabricated from SN88 silicon nitride manufactured by NGK Insulators, Ltd, Nagoya, Japan. Borescope inspections, which were conducted after shutdown cycles, revealed cracking after a 68 h engine test (Fig. 2). Selected vanes were sectioned for detailed SEM analysis. As shown in Fig. 3, a light-colored region or environment affected zone (EAZ) was found to have evolved in the vicinity of the primary crack. Subsequent indentation toughness measurements revealed that this zone exhibited a 3–5 times lower fracture toughness as compared with the bulk material. The asymmetry of the cracks extending from the corners of the Vickers indenter further suggested the presence of residual stress. Both of these observations may have been a factor in the formation of the microcracks along the airfoil surface. X-ray diffraction analyses
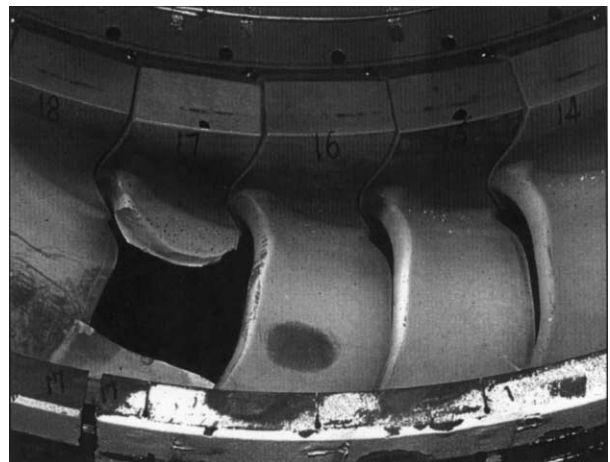

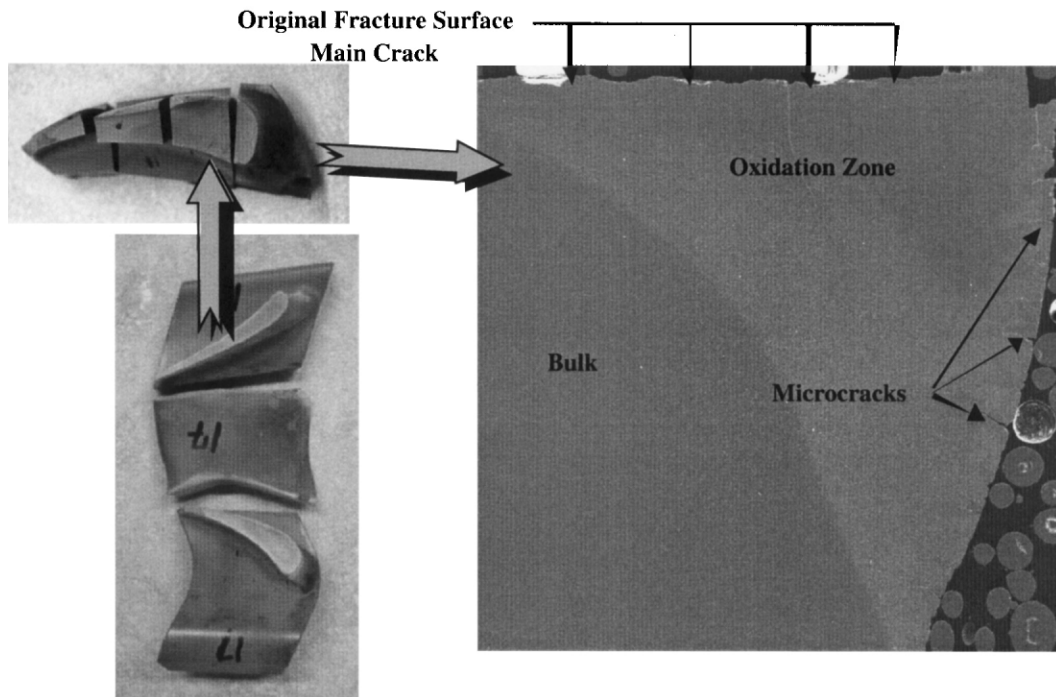Fig. 2. Nozzle assembly after 68 h test showing failed nozzle.

Fig. 3. Cross-section of failed nozzle showing damage zone evolution in the vicinity of the primary fracture surface. The light-colored zone was found to exhibit a higher oxygen content compared to the bulk material.

indicated that changes in the microstructure and secondary phase in the EAZ were due to the transformation of the secondary phase (J-phase—$Yb_4Si_2O_7N_2$) to $Yb_2Si_2O_7$ plus $Yb_2Si_2O_5$. The phase change from $Yb_4Si_2O_7N_2$ to $Yb_2Si_2O_7$ would result in 64% decrease in material volume, while the change from $Yb_4Si_2O_7N_2$ to $Yb_2Si_2O_5$ only causes a minor increase ($\sim$6%) in material volume. The substantial volume decrease associated with this phase transformation was responsible for the residual stress and reduction in fracture toughness. Based upon correlations of the fracture locations with the predicted temperature distributions via the finite element analysis, it was also concluded that formation of the EAZ occurred at a relatively low temperature (about 850 °C). Subsequent laboratory studies[5] showed that this behavior occurred as a result of the loss of the normally protective silica scale. Also, dynamic fatigue studies at intermediate temperatures in air indicated that the phase changes resulted in a substantial degradation in mechanical strength of SN88 silicon nitride.[5] This mechanical instability at intermediate temperatures was responsible for a significant susceptibility to slow crack growth, and thus, the fracture of SN88 silicon nitride nozzle during engine testing.

3.2. Rolls-Royce

The vanes examined in this program (Phase I) were fabricated from AS800 silicon nitride (Honeywell Ceramic Components, Torrance, CA).[2,16,17] The AS800,

densified using $\sim$10 wt.% rare-earth sintering aids, is classified as self-reinforced silicon nitride ceramic due to the presence of reinforcing elongated β-Si_3N_4 grains. The first stage ceramic vanes (Fig. 4) were designed for retrofit into a Model 501-K turbine, 3.1 MW engine (Rolls-Royce Allison, Indianapolis, IN). Following a 22 h shakedown run in a test turbine, the first stage vane assembly was mounted in a Model 501-K turbine at a commercial site (Exxon, Mobile, AL). During the field tests at Exxon, the average temperature and pressure of gas entering the vanes were approximately 1066 °C (1950 °F) and 8.9 atm (128 psia), respectively. These temperature and gas pressure data obtained were based on the finite element analyses carried out by Rolls-Royce Allison. However, due to the combustor temperature pattern, the mid-span gas temperature could have been as high as 1288 °C (2350 °F) at the "hot spot." The inlet gas velocity at vane mid-span was about 162 m/s (530 ft/s) and the gas accelerated to about 573 m/s (1880 ft/s) at the vane exit. Due to the extremely humid conditions during the test, the mole fraction of water vapor for the gas entering the vanes was calculated to be 0.101.

In Phase I, the AS800 silicon nitride vanes were evaluated without any protective coating. Although no vane failures occurred during the field test, dimensional measurements indicated that the AS800 silicon nitride vanes exhibited a significant material recession. Consequently, the engine test was terminated after 793 h engine test (815 h total time including shakedown test). As indicated in
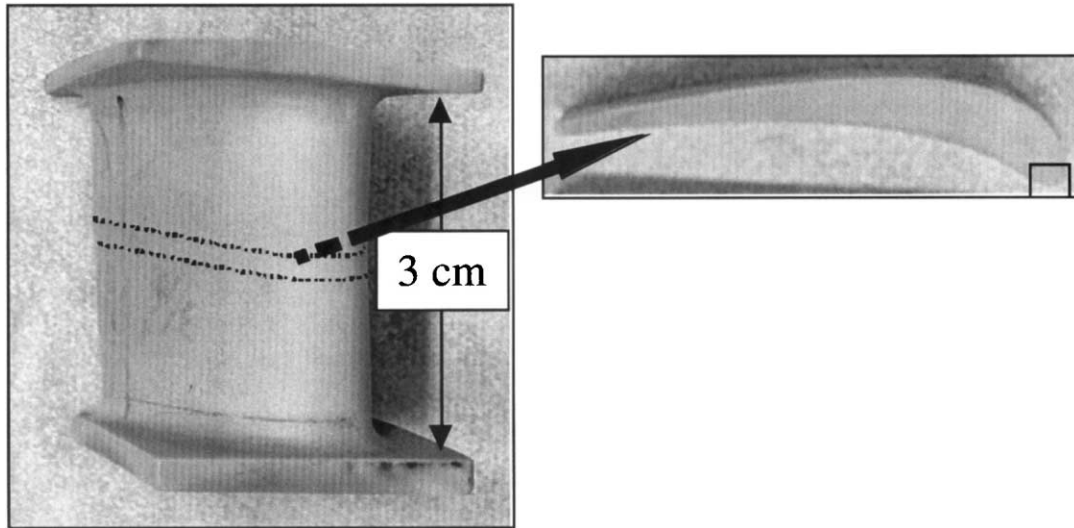
Fig. 4. Sectioning of vanes required for SEM of cross-sections.

Table 1
Summary of 815 h recession measurements and calculated temperatures

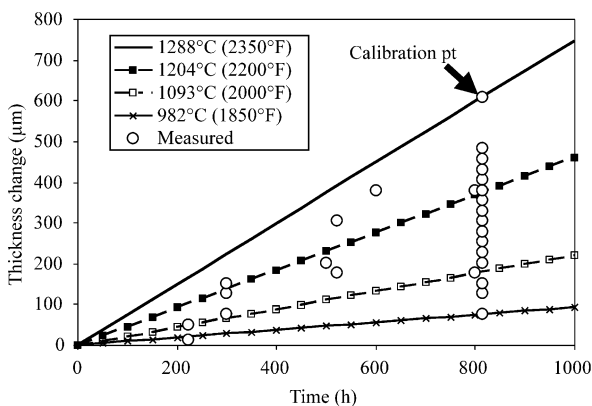| Vane no.	Recession (μm) at midspan of trailing edge after 815 h	T (°C)	T (°F)	Comments
3	76.2	983	1801	Calculated
5	127	1046	1915	Calculated
6	152.4	1070	1958	Calculated
8	203.2	1110	2031	Calculated
9	228.6	1127	2061	Calculated
10	254	1143	2089	Calculated
11	279.4	1158	2116	Calculated
12	304.8	1171	2140	Calculated
13	330.2	1184	2162	Calculated
14	355.6	1195	2184	Calculated
15	381	1207	2204	Calculated
16	406.4	1217	2223	Calculated
17	431.8	1228	2242	Calculated
18	457.2	1237	2259	Calculated
19	482.6	1246	2276	Calculated
24	609.6	1288	2350	Used to calibrate Eq. (1)

Fig. 5. Measurement of recession of the silicon nitride vanes at the mid-span of the trailing edge (open circles). The solid lines in this figure represent predictions based upon a model described in the Introduction.

Table 1, a few vanes were dimensionally inspected with a coordinate measuring machine (CMM).

Fig. 5 summarizes the thickness measurements obtained via the micrometer for the mid-span region of the trailing edge (symbols). Each data point represents a separate vane. The loss of material, which was excessive for a number of vanes, was due to the inability of the silicon nitride to retain a protective silica scale. In gas turbine environments, the silica reacts with water vapor to form gaseous $Si(OH)_4$, which is swept away by the high velocity gas. The competing processes of silica scale formation and scale volatilization ultimately lead to a steady-state value of the scale thickness as well as a linear recession of the ceramic substrate. Using the approach outlined in a previous study,[15] the steady-state thickness was predicted to be less than 1 μm for temperatures above 900 °C. SEM confirmed that during the engine tests little or no silica was retained on the vane airfoil surfaces.

The extensive scatter in the data shown in Fig. 5 is most likely a consequence of the vane-to-vane temperature variations arising from the combustor pattern. To assess the influence of these variations, the recession was calculated as a function of time and temperature for a constant pressure (8.9 atm) and velocity (573 m/s) using the modified form of Eq. (2),

$$k_l \ (\mu m/h) = B \exp(-108 \ kJ/mol/RT) v^{1/2} P_{total}^{3/2} \qquad (4)$$

where B is a constant. For the AS800 silicon nitride vanes, B was estimated by assuming that the maximum recession value measured at the midspan of the trailing edge after 815 h, and was associated with the vane subjected to the highest expected temperature of 2350 °F (1288 °C).[1] To verify the validity of this approach, the

_____
[1] The recession rate is calculated by dividing the measured recession by the total time of 815 h.

calibrated version of Eq. (3) was then used to calculate the temperatures for the remaining vanes based on the recession thickness. Table 1 summarizes the results. The calculated temperature range is quite close to that expected on the basis of finite element analysis. The predicted time and temperature dependencies of the midspan trailing edge recession (solid lines in Fig. 5) are also in good agreement with the experimental data.

Dimensional measurements of Vane No. 24 made with a coordinate measurement machine revealed significant material loss in the region of the leading edge. The excessive recession in the leading edge region, where the tangential velocity is low, appears to be in contradiction with the velocity dependence predicted by the model. To further investigate this effect Vane No. 24 was sectioned along the mid-span of airfoil and subsequently examined using SEM (Fig. 4). Fig. 6 compares the profile of the leading edge region in the as-received condition with that obtained after 815 h engine test. The applicability of the recession model to predict the change in profile was examined by using Eq. (1) to calculate the recession rate as function of position. The values of the pressure and velocity along the airfoil surface (required for this calculation) were obtained from the turbine manufacturer. These data were then used in conjunction with Eq. (3) to estimate the recession rate at each point along the airfoil surface. The change in the surface profile was calculated by assuming that the recession was normal to the surface at the point in question and that the magnitude was equal to the product of the rate and time. As shown in Fig. 6, the prediction profile (white dotted-line) for the 815 h vane in
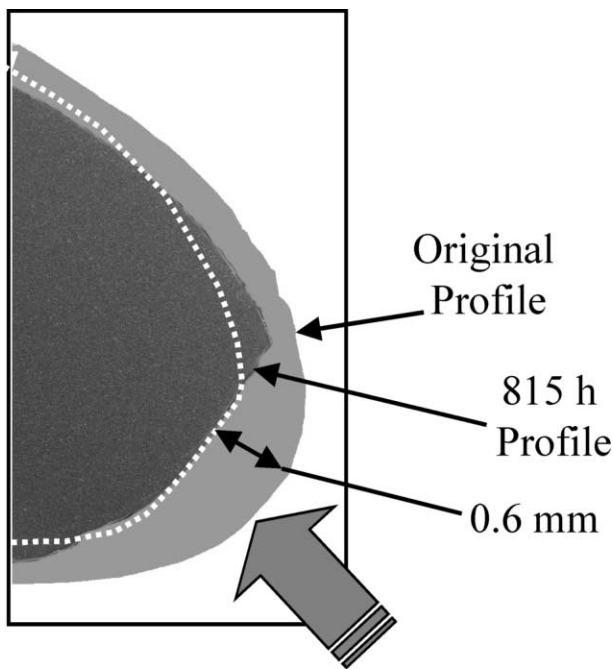
the leading edge region was in good agreement with the experimentally determined profile.

To further investigate the recession model, the loss of material along the trailing edge was measured for Vane No. 60. The temperature at each measurement point was determined from steady-state thermal analysis. Because of variations in combustion profiles, the temperature profiles varied with position. The trailing edge temperatures associated with the two extremes in temperature conditions were then used in conjunction with Eq. (3) to predict the recession. Fig. 7 compares the measured recession data with the two predicted profiles. Considering the uncertainty in the predicted temperature values, the agreement is fairly good. More importantly, the experimental recession profile exhibits a sharp maximum near the mid-span, which is similar to the predicted curves.

The strengths of the ceramic vanes from Phase I field test were measured using the ball-on-ring arrangement. The strength data are summarized in Fig. 8. The strengths of the specimens removed from the airfoil platform were consistently higher than those removed
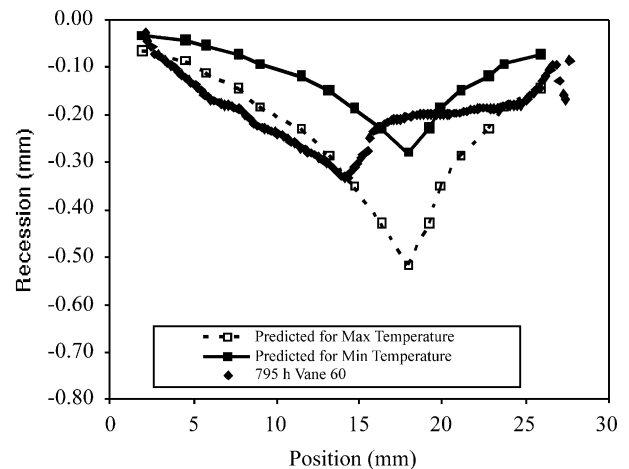
Fig. 7. Comparison of measured and predicted recession along the trailing edge.

Fig. 6. Profiles of leading edge (midspan) before testing and after 815 h. The large black arrow indicates gas flow direction.
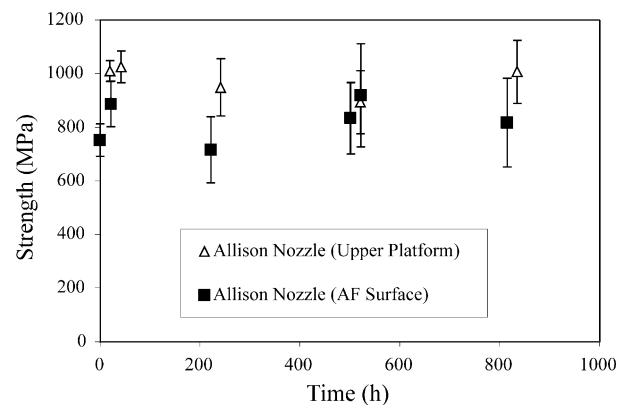
Fig. 8. Biaxial flexure strength data of AS800 vanes versus engine exposure time.

from the airfoil surface. This difference could in part be attributed to the development of a brittle zone due to attack from the gas turbine environments in the samples machined from the airfoil surfaces, as shown in Fig. 9. The depth of the brittle zone increased with an increase in exposure time up to 500 h, and then remained relatively constant ($\sim$55–60 μm) for exposure times greater than 500 h. The mechanical results also showed that there was a minor change in average strength with time, but there was an increase in the standard deviation in the strength of the specimens taken from the airfoil surfaces arising from the size variation of brittle zone developed. These results indicate that the strength of the airfoil surface was not significantly degraded by the material recession. This was in part due to the fact that
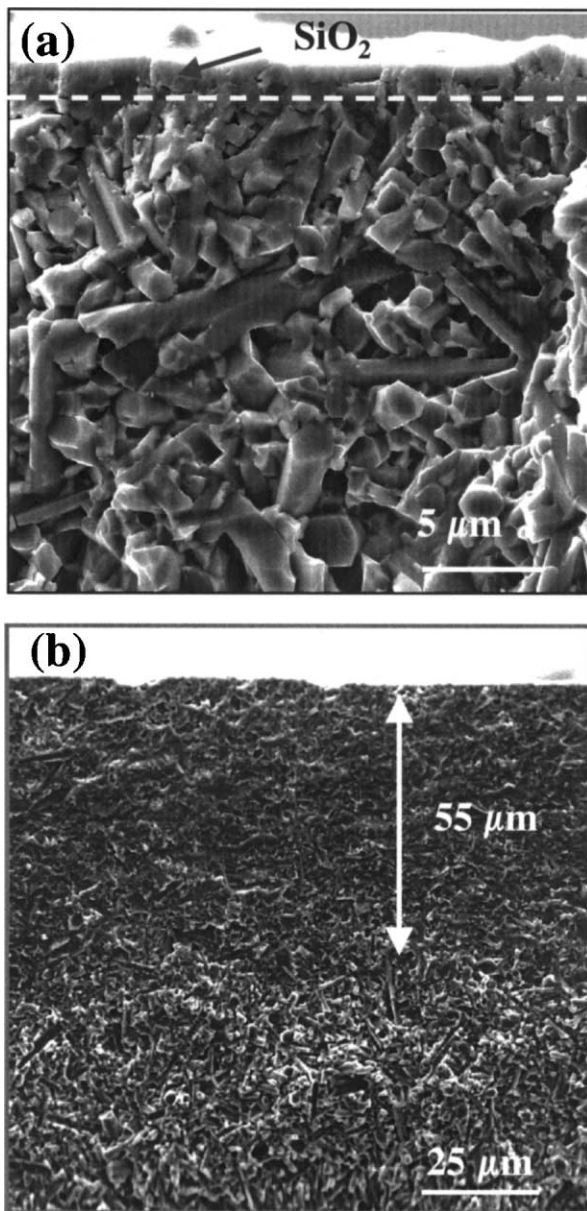
the silicon nitride material was continuously oxidized and removed by the high velocity gas and thus constantly exposed the bulk material to the gas turbine environments.

3.3. Pratt & Whitney

During the early 1990s Pratt & Whitney began developing an air-cooled silicon nitride turbine vane under funding provided by DARPA, US Department of Energy, Office of Industrial Technologies, and Office of Naval Research. The vane is designed to fit the Pratt & Whitney FT8 production engine, which is a 25.5 MW stationary engine derived from the JT8D flight engine. Because of the possible higher operating temperatures (1300 °C in the design at maximum steady state power condition), the air-cooled vane concept (Fig. 10) was adopted. A secondary benefit of the internal cooling scheme was that the outer surface would be subjected to a compressive stress state during operation. Note that the cooler inner surface would subject to a tensile stress state during operation.

In order to examine the mechanical consistency of an air-cooled SN282 silicon nitride vane, the miniature biaxial disk specimen was used to measure strength for specimens cut from the pressure (concave) and suction (convex) surfaces. For each surface three groups of specimens were fabricated: (1) inside surface machined; outer as-processed surface tested in tension (labeled outside), (2) outer surface machined; inner as processed surface tested in tension (labeled inside), and (3) both sides machined (labeled bulk). The results of these tests are summarized in Fig. 11. In general, the biaxial strength of SN282 silicon nitride vane strongly depended upon the sample location. For instance, the samples with as-processed surfaces machined from the pressure side exhibited higher strength than those machined front the suction side. Also, the strength values of the inside surfaces (particularly on the suction side) were well below those exhibited by the bulk material. This behavior could be attributed to the increased roughness as well as population of surface flaws on the inner surfaces arising from the green-state processing and bisque machining. These results indicate that the component

Fig. 9. Fracture surface of disk samples from airfoil surface of (a) as-received vane and (b) vane after 525 h engine test.
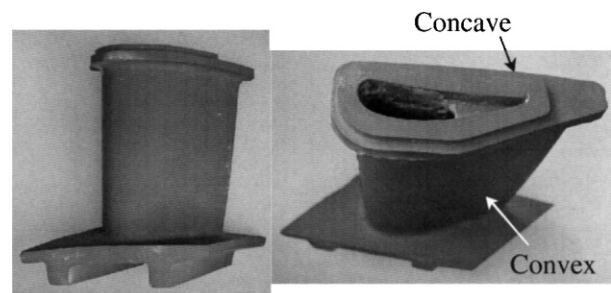
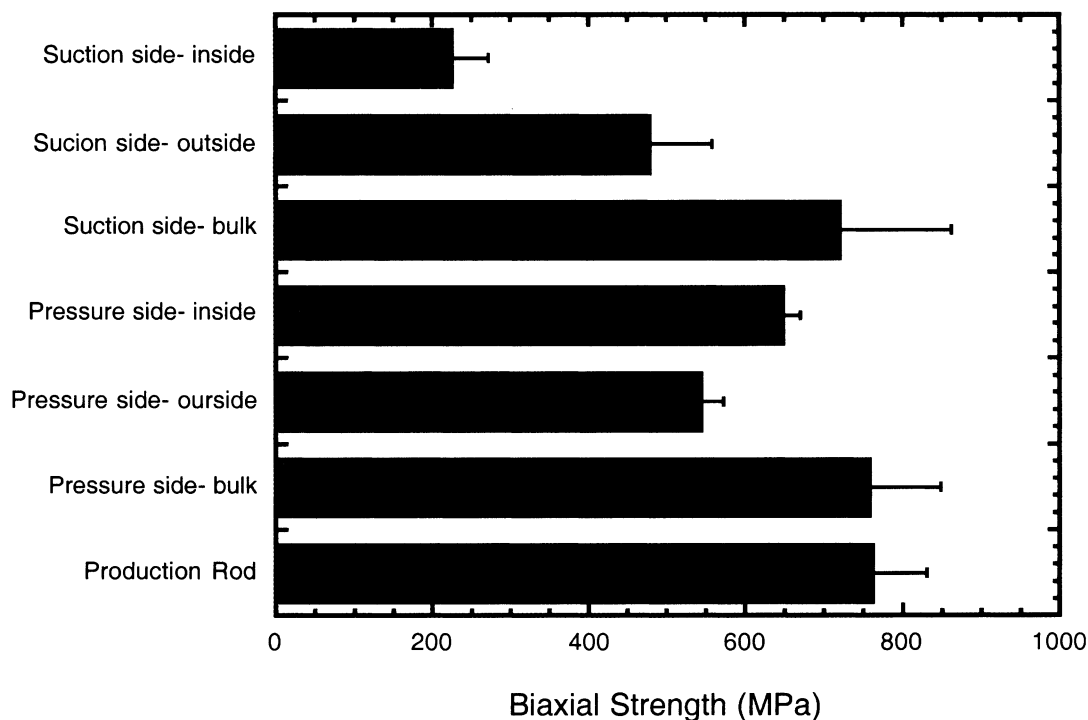Fig. 10. As manufactured FT8 air-cooled SN282 silicon nitride vane.

Fig. 11. Strength summary for samples extracted from the as-manufactured FT8 air-cooled SN282 silicon nitride vane.

reliability would be reduced significantly since during service the inner surfaces are subjected to residual tensile stresses.

4. Summary

A key lesson learned in this work is that mechanical properties of complex shaped ceramic components are often quite different from those determined from standardized simple-shaped test specimens. The application of component characterization can address this limitation by providing mechanical data directly from the ceramic components in question. Furthermore, evaluation of mechanical properties and microstructure as a function of engine test time can provide important insights into the effect of turbine environment upon the performance and reliability. Such insights are difficult and not feasible to be generated in a standard laboratory environment.

Characterization of ceramic components has also been instrumental in establishing recession data. Existing models, which account for the competitive effects of silica volatilization and silicon nitride oxidation provide an excellent description of the pressure, velocity, and temperature dependence of the material recession behavior. Characterization results suggested that environmental barrier coatings ultimately would be required to minimize this environmental effect and to ensure long-term stability and performance in gas turbine environments.

References

1. van Roode, M., Brentnall, W. D., Smith, K. O., Edwards, B. D., McClain, J. and Price, J. R., *Ceramic Stationary Gas Turbine Development—Fourth Annual Summary.* ASME paper 97-GT-317, presented at the International Gas Turbine and Aeroengine Congress and Exposition, Orlando, FL, 2–5 June 1997.
2. Wenglarz, R. A., Ali, S. and Layne, A., *Ceramics for ATS Industrial Turbines.* ASME Paper 96-GT-319, presented at the International Gas Turbine and Aeroengine Congress and Exposition, Birmingham, UK, 10–13 June 1996.
3. Holowczak, J. E., Bornemisza, T. G. and Day, W. H., Sector testing of cooled silicon nitride ceramic HPT vanes for the FT8 aeroderivative engine. In *Proceedings of the ASME TurboExpo 2000*, 8–11 May 2000 Munich, Germany, Paper Number 2000-GT-662.
4. Lin, H. T., Becher, P. F., Ferber, M. K. and Parthasarathy, V., Verification of creep performance of a ceramic gas turbine blade. *Key Engineering Materials*, 1999, **161–163**, 671–674.
5. Lin, H. T., Ferber, M. K. and van Roode, M., Evaluation of mechanical reliability of Si_3N_4 nozzles after exposure in an industrial gas turbine. In *Ceramic Materials and Components for Engines*, ed. J. G. Heinrich and A. Aldinger. Wiley-VCH, Weinheim/New York/Chicester/Brisbane/Singapore/Toronto, 2001, pp. 97–102.

6. Opila, E. J. and Hann, R. E. Jr., Paralinear oxidation of SiC in water vapor. *J. Am. Ceram. Soc.*, 1997, **80**(1), 197–205.

7. Opila, E. J., Variation of the oxidation rate of silicon carbide with vapor pressure. *J. Am. Ceram. Soc.*, 1999, **82**(3), 625–636.

8. Smialek, J. L., Robinson, R. C., Opila, E. J., Fox, D. S. and Jacobson, N., Recession due to SiO_2 scale volatility under combustor conditions. *Advanced Comp. Mater.*, 1999, **8**(1), 33–45.

9. Robinson, R. C. and Smialek, J. L., SiC recession caused by SiO_2 scale volatility under combustion conditions: I, experimental results and empirical model. *J. Am. Ceram. Soc.*, 1999, **82**(7), 1817–1825.

10. Opila, E. J., Smialek, J. L., Robinson, R. C., Fox, D. S. and Jacobson, N. S., SiC recession caused by SiO_2 scale volatility under combustion conditions: II, thermodynamics and gaseous-diffusion Model. *J. Am. Ceram. Soc.*, 1999, **82**(7), 1826–1834.

11. More, K. L., Tortorelli, P. F., Ferber, M. K. and Keiser, J. R., Observations of accelerated silicon carbide recession by oxidation at high water-vapor pressures. *J. Am. Ceram. Soc.*, 2000, **83**(1), 211–213.

12. Kirstein, A. F. and Woolley, R. M., Symmetrical bending of thin circular elastic plates on equally spaced point supports. *Journal of Research of the National Bureau of Standard—C. Engineering and Instrumentation*, 1967, **71C**(1).

13. Shetty, D. K., Rosenfield, A. R., McGuire, P., Bansal, B. K. and Duckworth, W. H., Biaxial flexure tests for ceramics. *Ceramic Bulletin*, 1980, **59**(12), 1193–1197.

14. Thiruvengadaswamy, R. and Scattergood, R. O., Biaxial flexure testing of brittle materials. *Scripta Metall. Mater.*, 1991, **25**, 2529–2532.

15. Brentnall, W. D., van Roode, M., Norton, P. F., Gates, S., Price, J. R., Jimenez, O. and Miriyala, N., Ceramic gas turbine development at Solar Turbines Incorporated. In *Progress in Ceramic Gas Turbine Development*, Vol. I. ed. M. van Roode, D. Richerson and M. K. Ferber. ASME Press.

16. Ferber, M. K., Lin, H. T., Parthasarathy, V., and Wenglarz, R. A., Characterization of silicon nitride vanes following exposure in an industrial gas turbine. Presented at IGTI Meeting in Munich, Germany, May 2000 (published as an ASME 2000-GT-631 pamphlet).

17. Ferber, M. K., Lin, H. T., and Keiser, J., Oxidation behavior of non-oxide ceramics in a high-pressure, high-temperature steam environment. In *Mechanical, Thermal and Environmental Testing and Performance of Ceramic Composites and Components (ASTM STP 1392)*, ed. M. G. Jenkins, E. Lara-Curzio and S. T. Gonczy. American Society for Testing and Materials, West Conshohocken, PA, 2000.